



Dual Specific Phosphatase 14 Deletion Rescues Retinal Ganglion Cells and Optic Nerve Axons after Experimental Anterior Ischemic Optic Neuropathy

Varun Kumar , Mohammad Ali Shariati , Louise Mesentier-Louro , Angela Jinsook Oh , Kristina Russano , Jeffrey L. Goldberg & Yaping Joyce Liao

To cite this article: Varun Kumar , Mohammad Ali Shariati , Louise Mesentier-Louro , Angela Jinsook Oh , Kristina Russano , Jeffrey L. Goldberg & Yaping Joyce Liao (2020): Dual Specific Phosphatase 14 Deletion Rescues Retinal Ganglion Cells and Optic Nerve Axons after Experimental Anterior Ischemic Optic Neuropathy, Current Eye Research, DOI: [10.1080/02713683.2020.1826976](https://doi.org/10.1080/02713683.2020.1826976)

To link to this article: <https://doi.org/10.1080/02713683.2020.1826976>



© 2020 The Author(s). Published with license by Taylor & Francis Group, LLC.



Published online: 27 Oct 2020.



Submit your article to this journal [↗](#)



Article views: 129




View related articles [↗](#)



View Crossmark data [↗](#)

Dual Specific Phosphatase 14 Deletion Rescues Retinal Ganglion Cells and Optic Nerve Axons after Experimental Anterior Ischemic Optic Neuropathy

Varun Kumar^{a,b}, Mohammad Ali Shariati^a, Louise Mesentier-Louro^a, Angela Jinsook Oh^a, Kristina Russano^a, Jeffrey L. Goldberg^a, and Yaping Joyce Liao^{a,c} 

^aSpencer Center for Vision Research, Byers Eye Institute, Palo Alto, California, USA; ^bSchepens Eye Research Institute, Massachusetts Eye and Ear, Department of Ophthalmology, Harvard Medical School, Harvard University, Boston, Massachusetts, USA; ^cDepartment of Neurology, Stanford University School of Medicine, Stanford, California, USA

ABSTRACT

Purpose: Understanding molecular changes is essential for designing effective treatments for nonarteritic anterior ischemic optic neuropathy (AION), the most common acute optic neuropathy in adults older than 50 years. We investigated changes in the mitogen-activated protein kinase (MAPK) pathway after experimental AION and focused on dual specificity phosphatase 14 (Dusp14), an atypical MAPK phosphatase that is downstream of Krüppel-like transcription factor (KLF) 9-mediated inhibition of retinal ganglion cell (RGC) survival and axonal regeneration.

Materials and methods: We induced severe AION in a photochemical thrombosis model in adult C57BL/6 wild-type and Dusp14 knockout mice. For comparison, some studies were performed using an optic nerve crush model. We assessed changes in MAPK pathway molecules using Western blot and immunohistochemistry, measured retinal thickness using optical coherence tomography (OCT), and quantified RGCs and axons using histologic methods.

Results: Three days after severe AION, there was no change in the retinal protein levels of MAPK ERK1/2, phosphorylated-ERK1/2 (pERK1/2), downstream effector Elk-1 and phosphatase Dusp14 on Western blot. Western blot analysis of purified RGCs after a more severe model using optic nerve crush also showed no change in Dusp14 protein expression. Because of the known importance of the Dusp14 and MAPK pathway in RGCs, we examined changes after AION in Dusp14 knockout mice. Three days after AION, Dusp14 knockout mice had significantly increased pERK1/2⁺, Brn3A⁺ RGCs on immunohistochemistry. Three weeks after AION, Dusp14 knockout mice had significantly greater preservation of retinal thickness, increased number of Brn3A⁺ RGCs on whole mount preparation, and increased number of optic nerve axons compared with wild-type mice.

Conclusions: Genetic deletion of Dusp14, a MAPK phosphatase important in KLF9-mediated inhibition of RGC survival, led to increased activation of MAPK ERK1/2 and greater RGC and axonal survival after experimental AION. Inhibiting Dusp14 or activating the MAPK pathway should be examined further as a potential therapeutic approach to treatment of AION.

Abbreviations: AION: anterior ischemic optic neuropathy; Dusp14: dual specific phosphatase 14; ERK1/2: extracellular signal-regulated kinases 1/2; Elk-1: ETS Like-1 protein; GCC: ganglion cell complex; GCL: ganglion cell layer; inner nuclear layer; KO: knockout; MAPK: mitogen-activated phosphokinase; OCT: optical coherence tomography; RGC: retinal ganglion cell; RNFL: retinal nerve fiber layer

ARTICLE HISTORY

Received 29 September 2019
Revised 2 September 2020
Accepted 15 September 2020

KEYWORDS

Dusp14; MAP kinase; AION; OCT; retinal ganglion cell; optic neuropathy

Introduction

Nonarteritic anterior ischemic optic neuropathy (AION) is the most common acute optic neuropathy in patients over 50 years, often resulting in permanent vision loss.^{1–4} This devastating condition typically presents as painless, sudden vision loss involving half (altitudinal, respecting the horizontal meridian) or more of the visual field in one eye, and the second eye is involved in 10.5–73% of patients.⁵ AION leads to irreversible loss of retinal ganglion cells (RGCs)^{6,7} and their axons in the retina and optic nerve, respectively.^{8,9} Despite its prevalence, the pathogenic mechanisms of AION and the subsequent events that lead to irreversible RGC loss and optic atrophy remain unclear.^{1,4,10} A better understanding the molecular changes in this disease may help identify potential treatments to protect or restore vision.

Although the molecular events following AION are not well understood, studies in glaucoma and optic nerve crush and transection models have implicated the mitogen-activated protein kinase (MAPK) family of serine/threonine-specific kinases in RGC survival and molecular signaling.^{11–13} MAPKs are also known to be important in retinal ischemia¹³ and stroke.^{14,15} The MAPK signaling pathway is important in RGC survival and is downstream of the neuroprotective effect of brain-derived neurotrophic factor (BDNF). BDNF binds to the tropomyosin receptor kinase (Trk) B receptor and stimulate multiple signaling pathways including phosphorylation and activation of ERK1/2.^{16,17} In glaucoma, overexpression of neurotrophins such as Brain Derived-Neurotrophic Factor (BDNF) and Ciliary Neurotrophic Factor (CNTF) protects RGCs.^{18–20}

MAPKs play essential roles in eukaryotic cells by transducing neighboring neurotrophic signals as well as environmental stress signals into cellular phenotypes.^{21–23} MAPKs are grouped into families, the extracellular signal regulated protein kinases (ERKs), the c-Jun N-terminal kinases (JNKs), and the p38 MAPKs; manipulation of any of these has been shown to improve RGC survival in various model systems.^{11,24,25} The MAPKs are activated by phosphorylation, and the magnitude and duration of MAPK activity are regulated by phosphatases, which turn off MAPK activity by dephosphorylation.²⁶ Recently, a family of transcription factors called Krüppel-like transcription factors (KLFs), whose inhibition promotes RGC survival and axonal regeneration,^{27–29} has been shown to exert its effect through a MAPK phosphatase, dual-specificity phosphatase 14 (Dusp14).²⁸ In cultured RGCs, KLF9 requires expression of Dusp14 to suppress RGC axon growth, and knockdown of Dusp14 activity *in vivo* using adeno-associated virus 2 short hairpin ribonucleic acid (AAV2-anti-Dusp14-shRNA) increased BDNF-induced pERK signaling, RGC survival, and the number and length of regenerating axons after optic nerve crush.²⁸

There is currently no effective treatment for AION, and an understanding of the molecular changes after AION can help identify important target in designing future therapeutics. Given the importance of MAPKs in experimental optic neuropathies and the known role of Dusp14 in RGC survival and axonal regeneration, we ask whether ERK1/2 and Dusp14 are altered in photochemical thrombosis model of AION. We also investigated the impact of Dusp14 knockout on RGC survival following optic nerve ischemia.

Methods

Animals

All animal care and experiments were performed in accordance with the ARVO Guide to Use of Animals in Ophthalmic and Vision Research and with approval from the Stanford University Administrative Panel on Laboratory Animal Care. Sprague-Dawley rats of either sex were obtained from Harlan Laboratories (Indianapolis, IN, USA). Adult wild-type C57BL/6 mice (Charles River, Hollister, CA) and Dusp14 knockout mice³⁰ (bred in house) of either sex were kept at constant temperature, with a 12-hour light/dark cycle, with food and water available *ad libitum*. To confirm Dusp14 knockout genotype, PCR and qPCR were performed using standard protocols on tail DNA and Dusp14-specific primers (Dusp14 forward: 5' TCGAGATCCC CAACTTCAAC 3'; Dusp14 reverse: 5' TGTCAGCCACAGTGT CAAAG 3'; TaqMan, ThermoFisher Scientific, Rockford, IL).

Photochemical thrombosis model of AION

In 8–10-week-old wild-type or Dusp14 knockout mice, we induced severe photochemical thrombosis in a well-established model of AION^{8,31,32} by increasing the number of laser spots used from 15 to 30. Briefly, mice were anesthetized by intraperitoneal injection of ketamine 50–100 mg/kg (Hospira, Inc., Lake Forest, IL, USA), xylazine 2–5 mg/kg

(Bedford Laboratories, Bedford, OH, USA) and buprenorphine 0.05 mg/kg (Bedford Laboratories). The pupils of anesthetized mice were pharmacologically dilated with 1% tropicamide (Alcon Laboratories Inc., Fort Worth, TX) and 2.5% phenylephrine hydrochloride (Akorn Inc, Lake Forest, IL). Intraperitoneal vein injection of rose bengal (1.25 mM in 150 μ l of phosphate-buffered saline (PBS), Sigma-Aldrich, St. Louis, MO) was followed by illumination with a frequency doubled Nd:YAG laser (400 μ m diameter, 50 mW, 1 s duration, 30 spots, PASCAL, OptiMedica, Santa Clara, CA) as source of focused, low intensity light.^{8,31,32} Rose bengal is photoactivated by low energy laser light and leads to singlet oxygen generation, platelet aggregation and thrombosis, while sparing nonvascular tissues.^{33,34} To control for variability within animals, AION eyes were compared against contralateral “control” eyes, although we do not rule out mild changes in these eyes as result of contralateral AION.

Optic nerve crush and RGC purification

Optic nerve crush was performed in fifteen 4-week-old rats under anesthesia with an intraperitoneal injection of ketamine hydrochloride, 60 mg/kg, and xylazine hydrochloride, 8 mg/kg body weight. Briefly, the left optic nerve was exposed and crushed with fine forceps (Dumont #5) 2 mm behind the globe for 10 seconds, while avoiding injury to the ophthalmic artery.²⁸ Postoperatively, animals were allowed to recover on a heating pad and were given subcutaneous injections of 0.1 mg/kg buprenorphine hydrochloride twice a day for 3 consecutive days to minimize discomfort. Three days after the surgery, animals were sacrificed, retinæ were isolated and pooled, and RGCs were purified from these pooled retinæ using Retinal Ganglion Cell Isolation Kit (Cat-130-096-209, Miltenyi Biotec Inc, Auburn CA). This kit utilizes CD90.1, a known RGC marker that is primarily expressed by RGCs but not photoreceptors. Nonneuronal CD90.1-expressing cells such as microglia and endothelial cells were depleted using biotinylated antibody. RGCs were further enriched and separated by magnetic separation columns as described in the kit. Purified RGCs were lysed in RIPA buffer and prepared for Western blot.

Western blot analysis of whole retinal lysate and purified RGCs

We assessed expression of ERK1/2, pERK1/2, Elk-1, and Dusp14 using Western blotting. We prepared whole retinal lysates from freshly dissected three pairs of eyes from mice three-days after AION using standard protocol followed in our publication.³⁵ Whole retinæ were lysed in RIPA buffer containing protease and phosphatase inhibitor cocktails (78442, Thermo Scientific, Rockford, IL) and homogenized with Wheaton tissue grinder (Millville, NJ). Very small amount of protein was derived from purified RGCs after optic nerve crush in rats, and the Western blot analysis only focused on Dusp14. Protein concentration was determined using micro BCA kit per manufacturer's instructions (Pierce, Rockford, IL). Equal amounts of protein

(30–40 µg) were loaded onto 4–12% mini-SDS-PAGE gel (Invitrogen) for gel electrophoresis and Western blotting.

We performed immunoblotting with antibodies against Dusp14 (1:1000, ab134265, Abcam, Cambridge, MA), pERK1/2 (1:1000, SAB4301578, Sigma -Aldrich, St Louis, MO), ERK1/2 (1:1000, 9102 Cell Signaling, Beverly, MA), Ets-like protein-1, Elk-1 (1:1000, ab131465, Abcam, Cambridge, MA), Glyceraldehyde 3-phosphate dehydrogenase, GAPDH (1:1000, 2118 Cell Signaling, Beverly, MA), cofilin (1:1000, 3318 Cell Signaling, Beverly, MA). Secondary antibodies included horse radish peroxidase (HRP)-conjugated goat anti-rabbit immunoglobulin G (IgG) (1:1000, 31460 Thermo Fisher Scientific, Rockford, IL), anti-mouse (1:1000, 31460 Thermo Fisher Scientific, Rockford IL) and donkey anti-goat (1:1000, ab97110, Abcam, Cambridge, MA). For internal standard, we used antibodies against cofilin or GAPDH, which are common protein standards. Internal control with the closest molecular weight to target proteins was used in each experiment. Positive bands on immunoblots were visualized using enhanced chemiluminescence (ECL kit, 32106 Thermo Fisher Scientific, Rockford, IL), imaged on LAS-3000 (Fujiform, Minato-Ku, Tokyo), and quantified using Image J (<http://imagej.nih.gov/>). In some experiments, liver from Dusp14 knockout and wild type mice were prepared and probed by anti-Dusp14 Western blot as above, to validate the antibody and to confirm loss of protein expression in the knockout mice.

Spectral-domain OCT imaging and data analysis

We performed serial *in vivo* imaging of WT and Dusp14 KO mice at baseline and 3 weeks after AION using spectral-domain optical coherence tomography (Spectralis HRA +OCT, Heidelberg Engineering, GmbH, Heidelberg, Germany),^{8,31,32} which utilized a superluminescent diode laser with average wavelength of 870 nm. We used the circular “RNFL” scan to obtain high-resolution imaging of the peripapillary retina and performed manual segmentation of the ganglion cell complex (GCC, which is the combined thickness of the retinal nerve fiber layer, ganglion cell layer, and the inner plexiform layer) as described previously.^{36,37} We used 3 weeks after AION as a time point because previous serial OCT measurements for 6 weeks after AION showed that there is little further thinning of GCC 3 weeks after AION.⁸ All segmentation was performed in a masked fashion by one investigator and visually confirmed by a second masked investigator as needed.

Immunohistochemistry

For whole mount immunostaining and RGC density quantification three weeks after AION, animals were perfusion-fixed in 4% paraformaldehyde (PFA). Eyes were enucleated and post-fixed in 4% PFA overnight. Whole mount retinæ were prepared and immunostained with anti-brain-specific homeobox/POU domain protein 3A (Brn3A) antibody. Briefly, retinæ were washed three times in washing buffer (0.5% Triton-X in phosphate-buffered saline (PBS) for 10 minutes each, blocked with 10% normal donkey serum for 1 hour, incubated with goat anti-Brn3A primary antibody

(1:500; catalog number Sc-31984; Santa Cruz Biotechnology, Inc. Dallas, Texas, USA), mixed in antibody dilution buffer (2% Triton-X in PBS and 5% normal donkey serum) overnight, washed 3 times 10 minutes each the next day, incubated with Alexa Fluor 568 donkey anti-goat IgG secondary antibody (1:500; catalog number A-11057; Invitrogen, Rockford, IL), washed three times in PBS for 10 minutes and mounted on glass slides with ProLong Gold Antifade Reagent (P36930, Invitrogen, Eugene, OR) and covered with Fisherbrand cover glasses (Thermo Fisher Scientific, Waltham, MA).

For immunostaining of frozen horizontal sections, whole eyes were fixed, cryoprotected with 30% sucrose, frozen on dry ice, and cut into 15-µm-thick retinal sections using cryostat (Model CM3050S, Buffalo Groove, IL). Retinal sections were rinsed in PBS and blocked and permeabilized in 20% normal goat serum with 0.02% Triton X-100 in antibody buffer (150 mM NaCl, 50 mM Tris base, 1% BSA, 0.04% sodium azide, pH 7.4) for an hour in room temperature to reduce non-specific binding. Samples were incubated with primary antibodies at 4°C overnight and then washed with PBS, incubated with secondary antibody for 2 hours at room temperature, washed with PBS, and mounted on glass slides with ProLong Gold Antifade Mountant with DNA stain DAPI. Primary antibodies used included anti-pERK1/2 (1:250, SAB4301578, Sigma-Aldrich, St Louis, MO), and anti-Brn3A (1:300, MAP 1585, Millipore, Billerica, MA). For secondary antibodies, we used highly cross-adsorbed Alexa Fluor-488 goat anti-rabbit IgG and Alexa Fluor-546 goat anti-mouse IgG antibodies (1:500, Invitrogen, Eugene, OR).

Morphometric analysis

To quantify RGC density, we imaged whole mount retinal preparations with an epifluorescence microscope (Nikon Eclipse TE300 microscope; Nikon Corp., Tokyo, Japan) using 20x objective. We took eight images per retina under masked condition, two images of 0.14 mm² from each quadrant, and calculated the number of Brn3A⁺ cells per image using a custom-written ImageJ script (ImageJ Macro, U.S. National Institutes of Health, Bethesda, MD), to calculate density of Brn3A⁺ cells/mm.² Each automatically performed cell count was visually reviewed under masked condition for quality control.

To quantify the number of pERK⁺Brn3A⁺ cells in the ganglion cell layer, we imaged immunostained frozen horizontal retinal sections near the optic nerve under masked conditions with confocal microscopy (Leica SP8 confocal microscope, IL, USA) using a 20x objective. To standardize retinal location, we imaged three to four high-power fields per slide using the same magnification 1–2.5 mm from the optic nerve head. Each high-power field was imaged in multiple channels with filter sets for each color, and images from each channel were quantified under masked conditions using ImageJ. The number of pERK1/2⁺Brn3A⁺ cells for each high-power field was normalized to the length of the ganglion cell layer counted and converted to pERK1/2⁺Brn3A⁺ cells/mm. For each data point, numbers from three to four images were averaged to calculate the value for each eye while masked, and

data for all the eyes were used to calculate mean and standard error of the mean.

Quantification of optic nerve axons

Three weeks after AION, we dissected the optic nerves for all animals and fixed in 4% PFA overnight to perform quantification of axon density. To standardize the portion of the optic nerve quantified, we analyzed the most anterior portion of the myelinated optic nerve, about 1 mm from the globe. Using an ultramicrotome (EM UC7, Leica, Wetzlar, Germany) we made multiple 1 μm transverse sections from each optic nerve (100 sections per eye) and stained them with 1% paraphenylenediamine (PPD) in methanol/isopropanol (1:1). The sections (9 sections per eye) were imaged at high-resolution in bright field using 100x objective (Nikon Eclipse TE300 microscope; Nikon Corp) and then tiled to cover the entire the optic nerve cross section. We manually counted the number of axons in two 22 μm \times 22 μm images per 4 quadrants of each optic nerve under masked condition and then calculated the density of each image and mean area density for each optic nerve as described.³⁸

Statistical analysis

All data were presented as mean \pm S.E.M. and analyzed using Graph Pad 7 (Prism, San Diego, USA). For statistical comparison of two sample groups, nonparametric Mann-Whitney U test was used, and $*p < .05$ was considered statistically significant. For groups of more than two, one-way analysis of

variance (ANOVA) was used with post-hoc Tukey multiple comparisons test.

Results

Stable expression of MAPK pathway molecules after AION

To examine changes in the MAPK pathway, we prepared whole retinal lysate from adult mice 3 days after severe AION and performed Western blot analysis (Figure 1a). Compared to control eyes, AION eyes had no change in the protein expression of phosphorylated ERK1/2 (pERK1/2) normalized to protein level of ERK1/2 ($n = 3$; $p = .94$). We also found that, after normalization against cofilin internal control, there was no change in the expression of ERK1/2 downstream target Elk-1 or MAPK phosphatase Dusp14 after AION ($n = 3$, $p = .43$; $n = 4$, $p = .97$ respectively).

Based on our previous finding that the MAPK phosphatase Dusp14 is particularly important in RGC survival after optic nerve crush model, we wondered whether the lack of change in Dusp14 expression was related to the AION model, which is relatively less severe than optic nerve crush, or due to the dilutional effect of non-RGC components of the retinal extract. Since MAPK pathway molecules have been known to be important in optic nerve crush model,³⁹ we performed optic nerve crush in 4-week-old rats and purified RGCs using well-known RGC marker CD90.1 (see Method). Western blot analysis of purified RGC protein extract after optic nerve crush showed that there was no change in Dusp14 expression after normalization with internal standard glyceraldehyde 3-phosphate dehydrogenase (GAPDH)⁴⁰ ($n = 3$, $p = .78$) (Figure 1b).

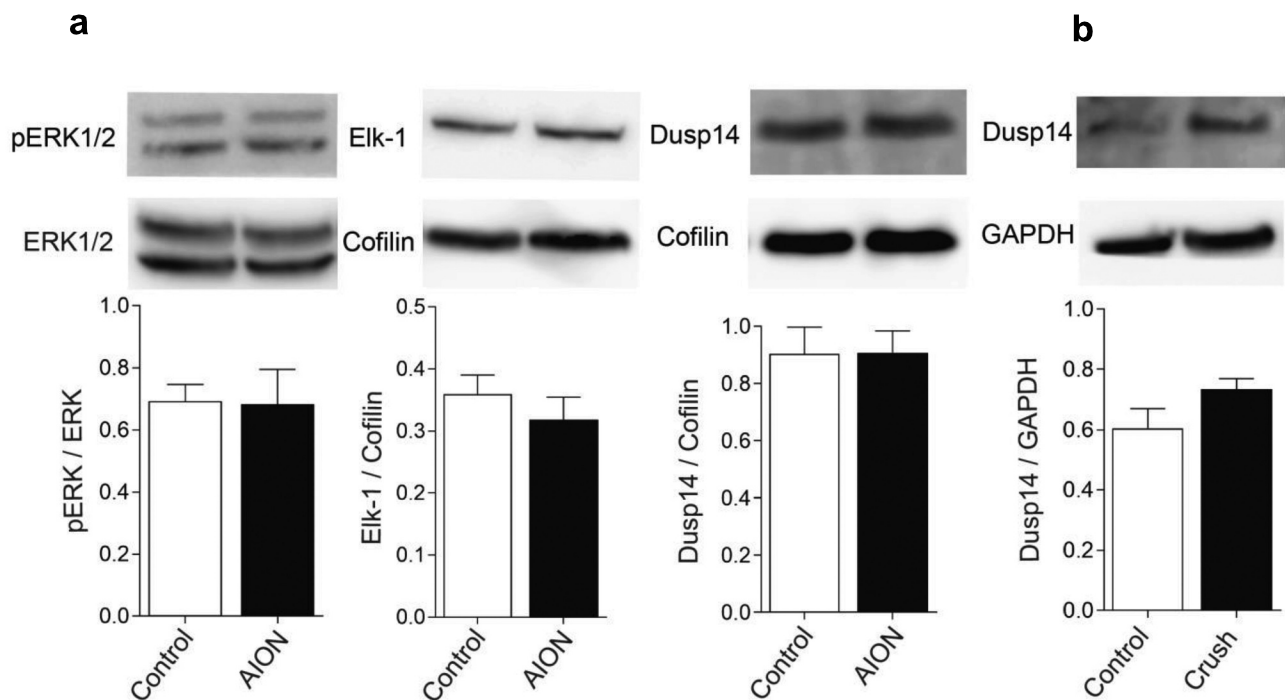


Figure 1. Western blot analysis of MAP kinase pathway molecules 3 days after photochemical thrombosis model of AION in mouse or 3 days after optic nerve crush in rats. (a) Representative Western blot (top) and quantification (bottom) of pERK1/2, ERK1/2, Elk-1, Dusp14, and cofilin (internal standard) in whole retinal lysate three days after AION in mouse. (b) Western blot analysis and quantification of Dusp14 and GAPDH (internal standard) in RGCs purified using RGC marker CD90.1 three days after optic nerve crush in rats.

Thus at least in the short-term measured in whole retinal lysates, Dusp14 expression and ERK expression and activation do not change in the acute period after AION, and RGC-specific Dusp14 expression does not change immediately after optic nerve crush.

Increased pERK1/2 in Brn3A⁺ RGCs after AION in Dusp14 knockout mice

Although there was no change in retinal Dusp14 expression in AION and optic nerve crush, knockdown of Dusp14 expression *in vivo* using AAV2-anti-Dusp14-shRNA was previously shown to promote RGC survival after optic nerve crush,²⁸ so we next asked whether lack of Dusp14 affects ERK1/2 expression³⁰ or activation or RGC survival after AION. We used Dusp14 knockout KO mice in order to ensure that our findings cannot be attributed to low level of Dusp14 expression or function in a viral vector-mediated knockdown model. Dusp14 KO mice was suitable for AION study because they survive to adulthood and breed with no difficulties, and have been found to have normal Brn3A⁺ RGC density.²⁸

We confirmed Dusp14 KO genotype using PCR, qPCR and Western blot (Figure 2a-c) and examined the expression of MAPK pathway molecules 3 days after AION. Using immunostaining of frozen horizontal sections, we found that there was a significant increase in the number of pERK1/2⁺ Brn3A⁺ cells in the ganglion cell layer in Dusp14 KO mice compared with WT mice ($n = 4$, $p = .029$, Mann-Whitney U test, Figure 2e,f). Western blot analysis of whole retinal lysate of WT and KO mice again showed no difference in expression of pERK1/2 normalized against cofilin ($n = 3$, $p = .99$, Figure 2g). Thus, Dusp14 plays a role in suppressing pERK1/2 after AION in RGCs, and RGC-specific immunostaining is a more sensitive method than whole-retinal Western blotting to detect these changes.

Increased RGC survival in Dusp14 knockout mice three-weeks after AION

To determine whether Dusp14 KO affected RGC survival after AION, we performed serial *in vivo* imaging using spectral-domain OCT (Figure 3a) and quantification of RGCs (Figure 3b) and optic nerve axons (Figure 3c) in Dusp14 KO and WT mice after AION. On OCT imaging 1 day after AION, there was an expected increase in ganglion cell complex (GCC) thickness in both WT and Dusp14 KO compared with control eyes (WT GCC day 0: 77 μ m; WT GCC day 1: 90.7 μ m $n = 4-7$; $p = .0001$; KO GCC day 0: 79.7 μ m; KO GCC day 1: 93.3 μ m: $n = 11$, $p = .0001$, one-way ANOVA post-hoc Tukey comparisons test) (Figure 3a) but no difference between WT and Dusp14 KO AION eyes ($p = .99$, one-way ANOVA post-hoc Tukey comparisons test). Twenty-one days after AION, when we expect to measure stable thinning of the GCC after AION,⁸ there was partial thinning of GCC in WT mice but not in Dusp14 KO at day 21 compared with day 0 (baseline ipsilateral eye) (WT GCC day 0: 77 μ m, day 21: 74.7 μ m; Dusp14 KO GCC day 0: 79.7 μ m, day 21: 79.4 μ m;) (Figure 3a). In summary, there

was 4.7 μ m thinning of GCC at day 21 compared to ipsilateral control eyes at day 0 in WT mice. However, there was 0.5 μ m thinning only in KO mice (Figure 3a), which is considered partial protection of GCC.

Quantification of Brn3A⁺ cells in retinal whole mount preparations confirmed that Dusp14 KO saved RGCs after AION. In WT mice 3 weeks after AION, there was a 60% reduction in Brn3A⁺ RGC area density in WT mice ($n = 7$; $p = .005$ Mann-Whitney U test) (Figure 3b). Compared with WT mice, Dusp14 KO mice had 17% greater preservation of RGC density ($n = 9$; $p = .005$ Mann-Whitney U test). This preservation of RGCs in Dusp14 KO is not due to increased RGC density of Dusp14 KO animals at baseline since we previously showed that Dusp14 KO had same Brn3A⁺ RGC density as WT mice.²⁸ Thus, although Dusp14 KO does not affect RGC viability during development, it is neuroprotective in this model of AION.

To assess optic nerve axonal density, we performed PPD axonal staining³⁸ 3 weeks after AION in WT and Dusp14 KO mice (Figure 3c). In Dusp14 KO mice, there was 45% greater preservation of optic nerve axonal area density compared with WT mice 3 weeks after AION ($n = 7$ for both; $p = .002$, Mann-Whitney U test). This 45% greater preservation of axons was more than the 17% preservation of Brn3A⁺ RGCs 3 weeks after AION, suggesting a greater impact of Dusp14 deletion on axonal survival compared with RGC soma survival.

Discussion

Dual specificity phosphatases like Dusp14 are important regulators of MAPK pathway – one of the most important signaling pathway in RGC survival and optic nerve regeneration – and they also play important roles in cellular response in cancer,⁴¹ infectious disease,⁴² or inflammatory disease.⁴³ We previously showed that AAV2-mediated Dusp14 knockdown rescues RGCs after optic nerve crush injury model²⁸ and in this study, we demonstrate for the first time that genetic deletion of Dusp14 rescues RGCs and preserved optic nerve axons after AION, the most common acute optic neuropathy in adults older than 50 years of age. We show that RGC rescue was associated with preservation of activated MAPK ERK1/2 in RGCs within 3 days after AION. We also show that the neuroprotective effect of Dusp14 deletion can be corroborated *in vivo* using OCT. This study is important because there is currently no effective treatment for AION, and we hope that better understanding of molecular changes after AION will lead to identification of novel therapeutics.

We previously demonstrated that AAV2-mediated Dusp14 knockdown protected RGCs one week after rat optic nerve crush injury and promoted limited axonal regeneration.²⁸ Dusp14 knockout also demonstrated significant RGC protection after optic nerve crush.²⁸ Despite the many differences between the AION and optic crush models, inhibition of Dusp14 and activation of ERK1/2 using genetic (this study) or viral²⁸ approaches rescues RGCs after optic nerve insult, suggesting a global role for Dusp14 in RGC death in optic neuropathies. Other Dusp family members such as Dusp6 and Dusp1 share homology with Dusp14, and in other model

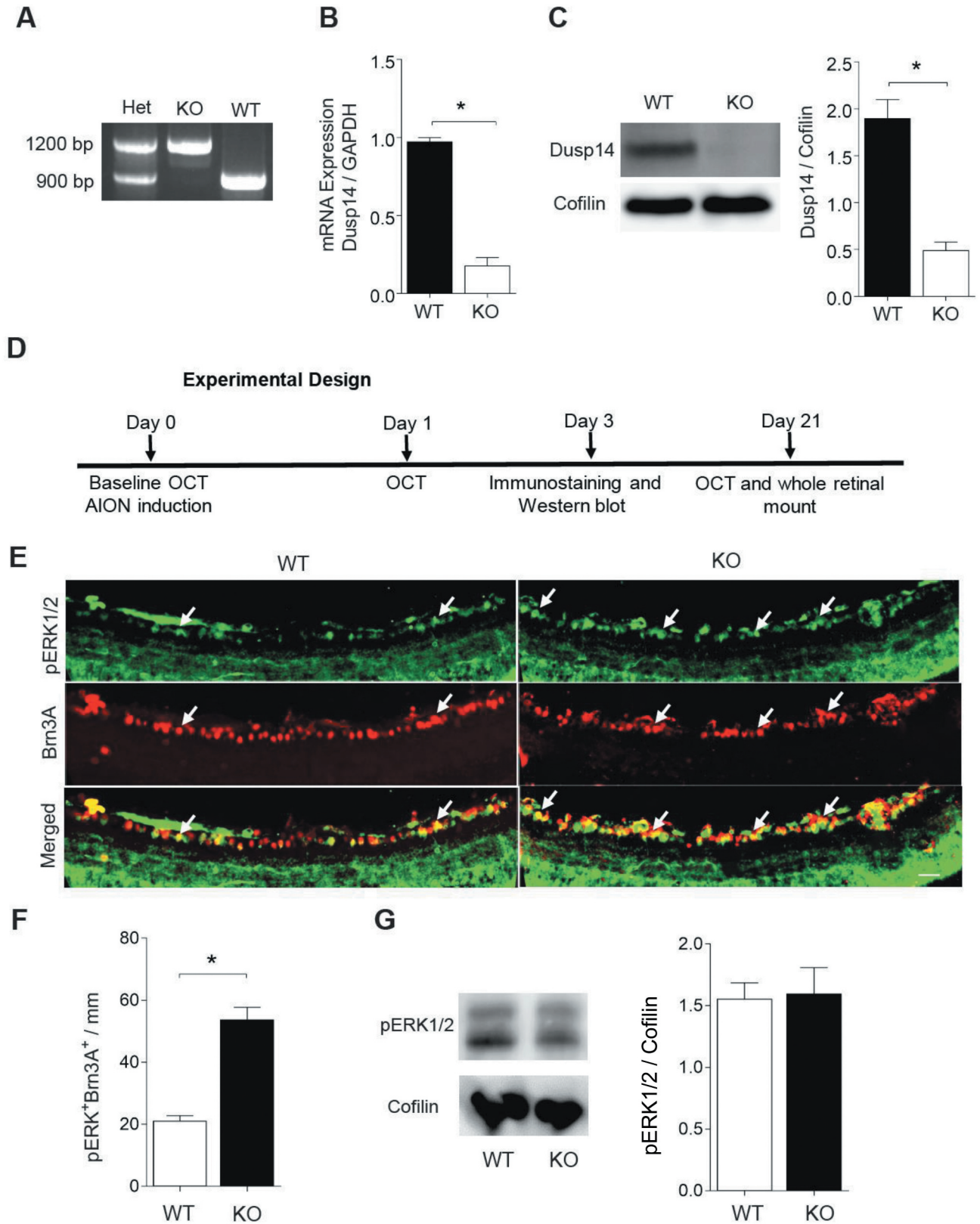


Figure 2. Characterization of Dusp14 knockout mouse and quantification of pERK1/2⁺ Brn3A⁺ RGCs 3 days after AION. (a) PCR genotyping of heterozygous (Het), C57BL/6 wild type (WT) and Dusp14 knockout (KO) mice. (b) mRNA expression of Dusp14 normalized to GAPDH in WT and KO mice ($n = 4$, $p = .02$, Mann-Whitney U test). (c) Western blot analysis of Dusp14 protein expression normalized to cofilin in WT and Dusp14 KO mice ($n = 3$, $*p = .02$, Mann-Whitney U test). (d) Experimental design of AION study. (e) Representative frozen horizontal retinal sections from WT and Dusp14 KO mice 3 days after AION immunostained with antibodies against pERK1/2 and Brn3A (scale bar: 25 μm). (f) Bar graph quantification of immunostaining showing significant relative preservation of pERK1/2⁺ Brn3A⁺ RGC in the ganglion cell layer in Dusp14 KO mice 3 days after AION ($n = 4$, $*p = .029$, Mann-Whitney U test) (g) Western blot example and quantification of whole retinal lysate Dusp14 KO had same pERK1/2 protein expression as WT 3 days after AION.

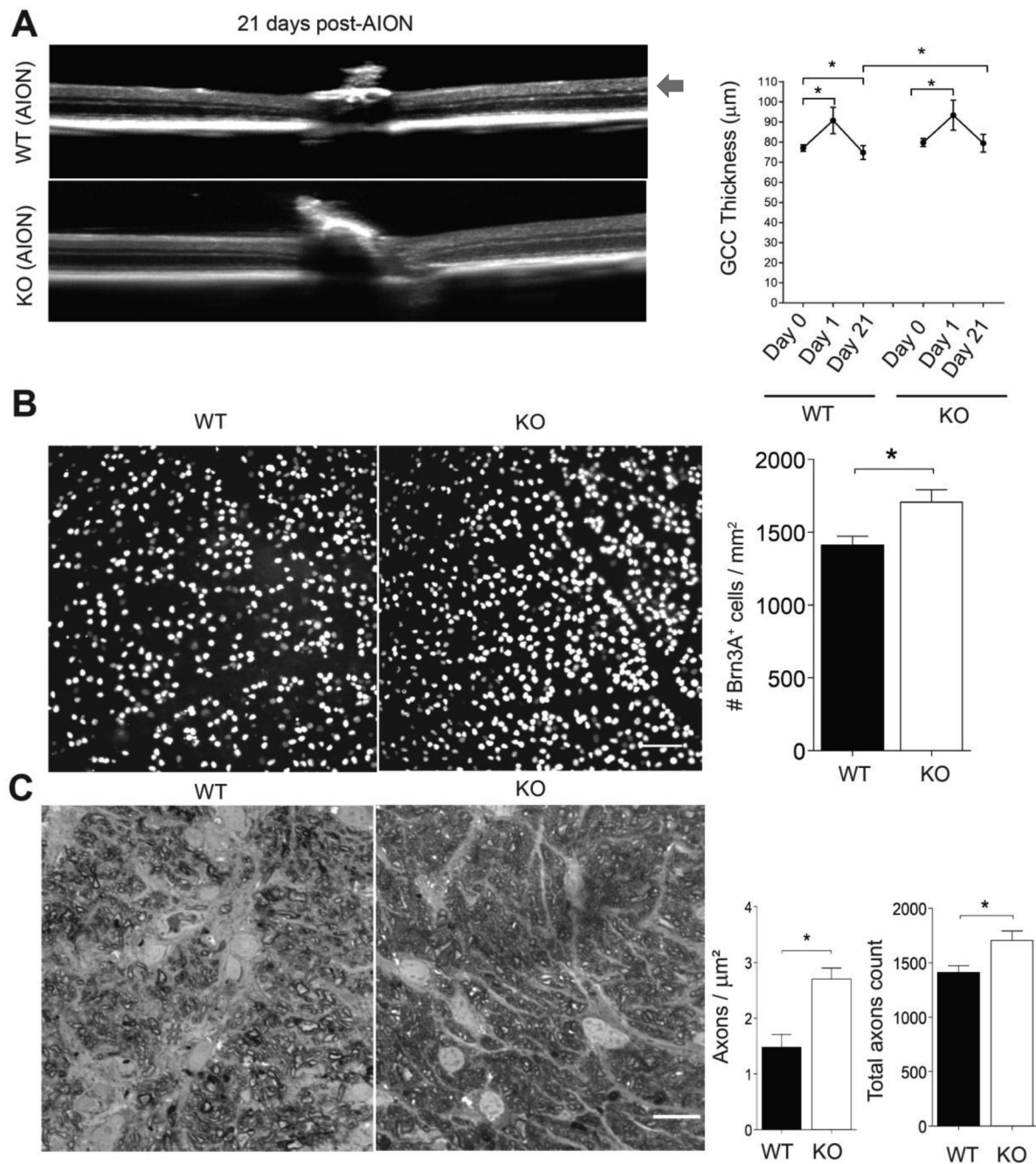


Figure 3. Dusp14 knockout mice demonstrate RGC neuroprotection and axon preservation 21 days after AION. (a) (Left) Representative images of OCT (line scan through optic disc) of wild type (WT) and Dusp14 knockout (KO) mice 21 days after AION. Temporal retina is on the left and nasal on the right of the images. Red arrow denotes ganglion cell complex (GCC). (Right) Bar graph of GCC thickness in WT and Dusp14 KO animals before AION (day 0) and at day 1 and day 21 after AION showing expected thickening of GCC at day 1 in both WT and Dusp14 KO groups and partial preservation of GCC thickness 3 weeks after AION in Dusp14 KO compared with WT ($*p = .0001$, one-way ANOVA with Tukey multiple comparisons test). (b) (Left) Representative images from retinal whole mount preparation stained with anti-Brn3A antibody from WT and Dusp14 KO mice 21 days after AION. Scale bar: 150 μm . (Right) Bar graph demonstrating significant preservation of Brn3A⁺ RGCs in Dusp14 KO mice compared with WT ($n = 9$; $*p = .005$ Mann-Whitney U test). (c) (Left) Representative optic nerve cross sections stained with axonal PPD staining in WT and Dusp14 KO mice 21 days after AION. WT sections had more gliosis (#) and swollen axons (\wedge). Scale Bar: 20 μm . (Right) Bar graph of quantification of axonal area density and total axonal count showing significant preservation of axonal density in Dusp14 KO mice compared to WT 3 weeks after AION ($n = 7$ for both; $*p = .002$, Mann-Whitney U test).

systems have been similarly linked to survival signaling. For example, embryonic fibroblasts from Dusp6 knockout mice have reduced apoptosis after myocardial infarction injury.⁴⁴

Previous study suggests that Dusp14 is mainly localized in RGCs pre- and post-optic nerve crush injury in rat.²⁸ However,

other similar Dusp family proteins such as Dusp1 (MKP1) are localized to other retinal cell types.⁴⁵

Upregulation of pERK1/2 in RGCs in various central nervous system injury models have been shown to be neuroprotective^{46–48} and important in neurotrophic factor-mediated pro-survival

signaling,^{46–48} including in RGCs after optic nerve injury in response to BDNF.²⁸ We showed that assessment of molecules in the MAPK pathway using Western blotting of whole retinal or RGC extracts is not a sensitive way of assessing the change in these molecules that result in saving RGCs or their axons in AION or optic nerve crush models. Instead, morphometric analysis using immunohistochemistry to examine pERK1/2⁺Brn3A⁺ cells in the ganglion cell layer is superior, and our data is consistent with activation of MAPK family member ERK1/2 in RGCs three days after AION in Dusp14 KO mice compared with control. As both kinases like ERKs and phosphatases like Dusp14 can be targeted pharmacologically or genetically, it would be interesting in future studies to determine whether additional synergy in neuroprotection can be elicited by targeting multiple enzymes in combination.

An important limitation of this study is the use of a genetic deletion model. It is scientifically important to assess the impact of complete elimination of Dusp14 expression, but there may be developmental impact of Dusp14 KO on the visual pathway and protein expression. Future AION studies using AAV-mediated knockdown of Dusp14 and comprehensive characterization of other MAPK family members can help confirm our findings in Dusp14 KO animals. For example, it will be important to characterize the role of other MAPK family members such as JNK and p38 in RGCs and in optic nerve axonal neuroprotection for Dusp14 knockout mice. Also, future work could be directed at characterizing the temporal expression profile of MAPK family members' expression and activation, which might be neuroprotective or detrimental depending on timing after ischemic insult. Finally, it will be important to extend these anatomic studies to functional assays, for example to investigate preservation of visual acuity in Dusp14 knockout mice after AION.

In conclusion, our study shows that inhibition of MAPK phosphatase Dusp14 rescued RGCs in AION, which is consistent with a model of disease where activation of MAPK phosphatase Dusp14 inhibits MAPK ERK1/2 and subsequent reduction in the survival of RGC soma and axon. Our study underscores the importance of studying cell-intrinsic negative regulators like Dusp14. Future studies of AION using Dusp deletion as well as cell type-specific Dusp14 knockdown or activation will help us better understand their functions and may lead to discovery of new therapies for treatment of optic neuropathies.

Acknowledgments

We thank Haoliang Huang, Ph.D. and Yang Hu, Ph.D. for help in optic nerve axon quantification.

Disclosure statement

The authors have no conflict of interest.

Funding

This work was supported by grants from the National Eye Institute (R01-EY022129; P30-EY026877), the Department of Defense CDMRP (JLG), and Research to Prevent Blindness grants (JLG) and by a NANOS Pilot Grant to YJL.

ORCID

Yaping Joyce Liao  <http://orcid.org/0000-0001-7958-291X>

References

- Hayreh SS. Anterior ischaemic optic neuropathy. Iii. Treatment, prophylaxis, and differential diagnosis. *Br J Ophthalmol.* 1974;58(12):981–89. doi:10.1136/bjo.58.12.981.
- Hayreh SS. Ischemic optic neuropathy. *Prog Retin Eye Res.* 2009;28(1):34–62. doi:10.1016/j.preteyeres.2008.11.002.
- Arnold AC. Pathogenesis of nonarteritic anterior ischemic optic neuropathy. *J Neuroophthalmol.* 2003;23(2):157–63. doi:10.1097/00041327-200306000-00012.
- Biousse V, Newman NJ. Ischemic optic neuropathies. *N Engl J Med.* 2015;373:1677.
- Beri M, Klugman MR, Kohler JA, Hayreh SS. Anterior ischemic optic neuropathy. Vii. Incidence of bilaterality and various influencing factors. *Ophthalmology.* 1987;94(8):1020–28. doi:10.1016/S0161-6420(87)33350-0.
- Slater BJ, Mehrabian Z, Guo Y, Hunter A, Bernstein SL. Rodent anterior ischemic optic neuropathy (raion) induces regional retinal ganglion cell apoptosis with a unique temporal pattern. *Invest Ophthalmol Vis Sci.* 2008;49(8):3671–76. doi:10.1167/iovs.07-0504.
- Zhang C, Guo Y, Slater BJ, Miller NR, Bernstein SL. Axonal degeneration, regeneration and ganglion cell death in a rodent model of anterior ischemic optic neuropathy (raion). *Exp Eye Res.* 2010;91(2):286–92. doi:10.1016/j.exer.2010.05.021.
- Ho JK, Stanford MP, Shariati MA, Dalal R, Liao YJ. Optical coherence tomography study of experimental anterior ischemic optic neuropathy and histologic confirmation. *Invest Ophthalmol Vis Sci.* 2013;54(9):5981–88. doi:10.1167/iovs.13-12419.
- Slater BJ, Vilson FL, Guo Y, Weinreich D, Hwang S, Bernstein SL. Optic nerve inflammation and demyelination in a rodent model of nonarteritic anterior ischemic optic neuropathy. *Invest Ophthalmol Vis Sci.* 2013;54(13):7952–61. doi:10.1167/iovs.13-12064.
- Levin LA, Danesh-Meyer HV. Hypothesis: A venous etiology for nonarteritic anterior ischemic optic neuropathy. *Arch Ophthalmol.* 2008;126(11):1582–85. doi:10.1001/archoph.126.11.1582.
- Zhou Y, Pernet V, Hauswirth WW, Di Polo A. Activation of the extracellular signal-regulated kinase 1/2 pathway by aav gene transfer protects retinal ganglion cells in glaucoma. *Mol Ther.* 2005;12(3):402–12. doi:10.1016/j.ymthe.2005.04.004.
- Fujita Y, Sato A, Yamashita T. Brimonidine promotes axon growth after optic nerve injury through erk phosphorylation. *Cell Death Dis.* 2013;4(e763). doi:10.1038/cddis.2013.298.
- Roth S, Shaikh AR, Hennelly MM, Li Q, Bindokas V, Graham CE. Mitogen-activated protein kinases and retinal ischemia. *Invest Ophthalmol Vis Sci.* 2003;44:5383–95.
- Sun J, Nan G. The mitogen-activated protein kinase (mapk) signaling pathway as a discovery target in stroke. *J Mol Neurosci.* 2016;59(1):90–98. doi:10.1007/s12031-016-0717-8.
- Sawe N, Steinberg G, Zhao H. Dual roles of the mapk/erk1/2 cell signaling pathway after stroke. *J Neurosci Res.* 2008;86(8):1659–69. doi:10.1002/jnr.21604.
- Liu Y, Tao L, Fu X, Zhao Y, Xu X. Bdnf protects retinal neurons from hyperglycemia through the trkb/erk/mapk pathway. *Mol Med Rep.* 2013;7(6):1773–78. doi:10.3892/mmr.2013.1433.
- Hu Y, Cho S, Goldberg JL. Neurotrophic effect of a novel trkb agonist on retinal ganglion cells. *Invest Ophthalmol Vis Sci.* 2010;51:1747–54.
- Almasieh M, Wilson AM, Morquette B, Cueva Vargas JL, Di Polo A. The molecular basis of retinal ganglion cell death in glaucoma. *Prog Retin Eye Res.* 2012;31(2):152–81. doi:10.1016/j.preteyeres.2011.11.002.
- Feng L, Chen H, Yi J, Troy JB, Zhang HF, Liu X. Long-term protection of retinal ganglion cells and visual function by brain-derived neurotrophic factor in mice with ocular

- hypertension. *Invest Ophthalmol Vis Sci.* 2016;57(8):3793–802. doi:10.1167/iovs.16-19825.
20. Pease ME, Zack DJ, Berlinicke C, Bloom K, Cone F, Wang Y, Klein RL, Hauswirth WW, Quigley HA. Effect of cntf on retinal ganglion cell survival in experimental glaucoma. *Invest Ophthalmol Vis Sci.* 2009;50(5):2194–200. doi:10.1167/iovs.08-3013.
 21. Robinson MJ, Cobb MH. Mitogen-activated protein kinase pathways. *Curr Opin Cell Biol.* 1997;9(2):180–86. doi:10.1016/S0955-0674(97)80061-0.
 22. Tan Z, Chang X, Puga A, Xia Y. Activation of mitogen-activated protein kinases (mapks) by aromatic hydrocarbons: role in the regulation of aryl hydrocarbon receptor (ahr) function. *Biochem Pharmacol.* 2002;64(5–6):771–80. doi:10.1016/S0006-2952(02)01138-3.
 23. Cowan KJ, Storey KB. Mitogen-activated protein kinases: new signaling pathways functioning in cellular responses to environmental stress. *J Exp Biol.* 2003;206(Pt 7):1107–15. doi:10.1242/jeb.00220.
 24. Kim BJ, Silverman SM, Liu Y, Wordinger RJ, Pang IH, Clark AF. In vitro and in vivo neuroprotective effects of cjun n-terminal kinase inhibitors on retinal ganglion cells. *Mol Neurodegener.* 2016;11(30). doi:10.1186/s13024-016-0093-4.
 25. Kikuchi M, Tenneti L, Lipton SA. Role of p38 mitogen-activated protein kinase in axotomy-induced apoptosis of rat retinal ganglion cells. *J Neurosci.* 2000;20(13):5037–44. doi:10.1523/JNEUROSCI.20-13-05037.2000.
 26. Kondoh K, Nishida E. Regulation of map kinases by map kinase phosphatases. *Biochim Biophys Acta.* 2007;1773(8):1227–37. doi:10.1016/j.bbamcr.2006.12.002.
 27. Apará A, Galvaó J, Wang Y, Blackmore M, Trillo A, Iwao K, Brown DP Jr., Fernandes KA, Huang A, Nguyen T, et al. Klf9 and jnk3 interact to suppress axon regeneration in the adult CNS. *J Neurosci.* 2017;37(40):9632–44. doi:10.1523/JNEUROSCI.0643-16.2017.
 28. Galvaó J, Iwao K, Apará A, Wang Y, Ashouri M, Shah TN, Blackmore M, Kunzevitzky NJ, Moore DL, Goldberg JL. The kruppel-like factor gene target *dusp14* regulates axon growth and regeneration. *Invest Ophthalmol Vis Sci.* 2018;59(7):2736–47. doi:10.1167/iovs.17-23319.
 29. Moore DL, Blackmore MG, Hu Y, Kaestner KH, Bixby JL, Lemmon VP, Goldberg JL. Klf family members regulate intrinsic axon regeneration ability. *Science.* 2009;326(5950):298–301. doi:10.1126/science.1175737.
 30. Yang CY, Li JP, Chiu LL, Lan JL, Chen DY, Chuang HC, Huang CY, Tan TH. Dual-specificity phosphatase 14 (*dusp14*/mcp6) negatively regulates tcr signaling by inhibiting tab1 activation. *J Immunol.* 2014;192(4):1547–57. doi:10.4049/jimmunol.1300989.
 31. Yu C, Ho JK, Liao YJ. Subretinal fluid is common in experimental non-arteritic anterior ischemic optic neuropathy. *Eye (Lond).* 2014;28(12):1494–501. doi:10.1038/eye.2014.220.
 32. Shariati MA, Park JH, Liao YJ. Optical coherence tomography study of retinal changes in normal aging and after ischemia. *Invest Ophthalmol Vis Sci.* 2015;56(5):2790–97. doi:10.1167/iovs.14-15145.
 33. Bernstein SL, Guo Y, Kelman SE, Flower RW, Johnson MA. Functional and cellular responses in a novel rodent model of anterior ischemic optic neuropathy. *Invest Ophthalmol Vis Sci.* 2003;44(10):4153–62. doi:10.1167/iovs.03-0274.
 34. Goldenberg-Cohen N, Guo Y, Margolis F, Cohen Y, Miller NR, Bernstein SL. Oligodendrocyte dysfunction after induction of experimental anterior optic nerve ischemia. *Invest Ophthalmol Vis Sci.* 2005;46(8):2716–25. doi:10.1167/iovs.04-0547.
 35. Kumar V, Mesentier-Louro LA, Oh AJ, Heng K, Shariati MA, Huang H, Hu Y, Liao YJ. Increased ER stress after experimental ischemic optic neuropathy and improved RGC and oligodendrocyte survival after treatment with chemical chaperon. *Invest Ophthalmol Vis Sci.* 2019;60(6):1953–66. doi:10.1167/iovs.18-24890.
 36. Nakano N, Ikeda HO, Hangai M, Muraoka Y, Toda Y, Kakizuka A, Yoshimura N. Longitudinal and simultaneous imaging of retinal ganglion cells and inner retinal layers in a mouse model of glaucoma induced by n-methyl-D-aspartate. *Invest Ophthalmol Vis Sci.* 2011;52(12):8754–62. doi:10.1167/iovs.10-6654.
 37. Hein K, Gadjanski I, Kretschmar B, Lange K, Diem R, Sattler MB, Bahr M. An optical coherence tomography study on degeneration of retinal nerve fiber layer in rats with autoimmune optic neuritis. *Invest Ophthalmol Vis Sci.* 2012;53(1):157–63. doi:10.1167/iovs.11-8092.
 38. Huang H, Miao L, Liang F, Liu X, Xu L, Teng X, Wang Q, Ridder WH 3rd, Shindler KS, Sun Y, et al. Neuroprotection by eIF2 α -chop inhibition and xbp-1 activation in EAE/optic neuritis. *Cell Death Dis.* 2017;8(7):e2936. doi:10.1038/cddis.2017.329.
 39. Mammone T, Chidlow G, Casson RJ, Wood JPM. Expression and activation of mitogen-activated protein kinases in the optic nerve head in a rat model of ocular hypertension. *Mol Cell Neurosci.* 2018;88(270–291). doi:10.1016/j.mcn.2018.01.002.
 40. Hollander A, D'Onofrio PM, Magharious MM, Lysko MD, Koeberle PD. Quantitative retinal protein analysis after optic nerve transection reveals a neuroprotective role for hepatoma-derived growth factor on injured retinal ganglion cells. *Invest Ophthalmol Vis Sci.* 2012;53(7):3973–89. doi:10.1167/iovs.11-8350.
 41. Lawan A, Al-Harhi S, Cadalbert L, McCluskey AG, Shweash M, Grassia G, Grant A, Boyd M, Currie S, Plevin R. Deletion of the dual specific phosphatase-4 (*dusp-4*) gene reveals an essential non-redundant role for map kinase phosphatase-2 (*mcp-2*) in proliferation and cell survival. *J Biol Chem.* 2011;286(15):12933–43. doi:10.1074/jbc.M110.181370.
 42. Vandereyken MM, Singh P, Wathieu CP, Jacques S, Zurashvili T, Dejager L, Amand M, Musumeci L, Singh M, Moutschen MP, et al. Dual-specificity phosphatase 3 deletion protects female, but not male, mice from endotoxemia-induced and polymicrobial-induced septic shock. *J Immunol.* 2017;199(7):2515–27. doi:10.4049/jimmunol.1602092.
 43. Vattakuzhi Y, Abraham SM, Freidin A, Clark AR, Horwood NJ. Dual-specificity phosphatase 1-null mice exhibit spontaneous osteolytic disease and enhanced inflammatory osteolysis in experimental arthritis. *Arthritis Rheum.* 2012;64(7):2201–10. doi:10.1002/art.34403.
 44. Maillet M, Purcell NH, Sargent MA, York AJ, Bueno OF, Molkentin JD. *Dusp6* (*mcp3*) null mice show enhanced erk1/2 phosphorylation at baseline and increased myocyte proliferation in the heart affecting disease susceptibility. *J Biol Chem.* 2008;283(45):31246–55. doi:10.1074/jbc.M806085200.
 45. Dreixler JC, Bratton A, Du E, Shaikh AR, Savoie B, Alexander M, Marcet MM, Roth S. Mitogen-activated protein kinase phosphatase-1 (*mcp-1*) in retinal ischemic preconditioning. *Exp Eye Res.* 2011;93(4):340–49. doi:10.1016/j.exer.2010.10.011.
 46. Hetman M, Kanning K, Cavanaugh JE, Xia Z. Neuroprotection by brain-derived neurotrophic factor is mediated by extracellular signal-regulated kinase and phosphatidylinositol 3-kinase. *J Biol Chem.* 1999;274(32):22569–80. doi:10.1074/jbc.274.32.22569.
 47. Sun X, Zhou H, Luo X, Li S, Yu D, Hua J, Mu D, Mao M. Neuroprotection of brain-derived neurotrophic factor against hypoxic injury in vitro requires activation of extracellular signal-regulated kinase and phosphatidylinositol 3-kinase. *Int J Dev Neurosci.* 2008;26(3–4):363–70. doi:10.1016/j.ijdevneu.2007.11.005.
 48. Wu H, Yang SF, Dai J, Qiu YM, Miao YF, Zhang XH. Combination of early and delayed ischemic postconditioning enhances brain-derived neurotrophic factor production by upregulating the erk-creb pathway in rats with focal ischemia. *Mol Med Rep.* 2015;12(5):6427–34. doi:10.3892/mmr.2015.4327.